Journal Pre-proof

The influence of lens position, vault prediction, and posterior cornea on phakic posterior chamber intraocular lens power.

Jascha A. Wendelstein , Tun Kuan Yeo , Sarah Hinterberger , Theo G. Seiler , H Burkhard Dick , Giacomo Savini , Achim Langenbucher , Suphi Taneri

PII: S0002-9394(24)00011-4
DOI: https://doi.org/10.1016/j.ajo.2024.01.008
Reference: AJOPHT 12769

To appear in: *American Journal of Ophthalmology*

Received date: October 31, 2023
Revised date: January 4, 2024
Accepted date: January 5, 2024

Please cite this article as: Jascha A. Wendelstein , Tun Kuan Yeo , Sarah Hinterberger , Theo G. Seiler , H Burkhard Dick , Giacomo Savini , Achim Langenbucher , Suphi Taneri , The influence of lens position, vault prediction, and posterior cornea on phakic posterior chamber intraocular lens power., *American Journal of Ophthalmology* (2024), doi: https://doi.org/10.1016/j.ajo.2024.01.008

The influence of lens position, vault prediction, and posterior cornea on phakic posterior chamber intraocular lens power.

Short Title: Effective lens position in phakic intraocular lenses

Jascha A. Wendelstein[1,2,3,4], Tun Kuan Yeo[5], Sarah Hinterberger[1,2], Theo G. Seiler[3,6,7], H Burkhard Dick[8], Giacomo Savini[9], Achim Langenbucher[4], Suphi Taneri[8,10]

1. Johannes Kepler University Linz, Medical Faculty, Altenberger Strasse 69, 4040 Linz, Austria
2. Department for Ophthalmology and Optometry, Kepler University Hospital GmbH, Krankenhausstrasse 9, 4020 Linz, Austria
3. Institut für Refraktive und Ophthalmo-Chirurgie (IROC), Zurich, Switzerland
4. Institute of Experimental Ophthalmology, Saarland University, Kirrberger Str. 100/22, 66424 Homburg, Germany
5. Tan Tock Seng Hospital, Singapore
6. Universitätsklinik für Augenheilkunde, Inselspital Bern, Bern, Switzerland
7. Klinik für Augenheilkunde, Universitätsklinikum Düsseldorf, Duesseldorf, Germany
8. Department of Ophthalmology, University of Bochum, Bochum, Germany.
9. IRCCS – Fondazione Bietti, Rome, Italy
10. Zentrum für Refraktive Chirurgie, Muenster, Germany.

Corresponding author: Jascha Wendelstein

Johannes Kepler University Linz, Medical Faculty, Altenberger Strasse 69, 4040 Linz, Austria

Department for Ophthalmology and Optometry, Kepler University Hospital GmbH, Krankenhausstrasse 9, 4020 Linz, Austria

IROC – Institut für Refraktive- und Ophthalmo-Chirurgie Zürich Stockerstrasse 37, CH-8002 Zürich, Switzerland

Institute of Experimental Ophthalmology, Saarland University, Kirrberger Str. 100/22, 66424 Homburg, Germany

wendelsteinjascha@gmail.com

Phone: +43 (0)5 7680 83 – 1048

Fax: +43 (0)5 7680 83 – 1822

Abstract:

Background: Achieving precise refractive outcomes in phakic posterior chamber intraocular lens (pIOL) implantation is crucial for patient satisfaction. This study investigates factors affecting pIOL power calculations, focusing on myopic eyes, and evaluates the potential benefits of advanced predictive models.

Design: Retrospective, single-center, algorithm improvement study

Methods: Various variations with different effective lens position (ELP) algorithms were analyzed. The algorithms included a fixed constant model, and a multiple linear regression model and were tested with and without incorporation of the posterior corneal curvature (Rcp). Furthermore, the impact of inserting the postoperative vault, the space between the pIOL and the crystalline lens, into the ELP algorithm was examined, and a simple vault prediction model was assessed.

Results: Integrating Rcp and the measured vault into pIOL calculations did not significantly improve accuracy. Transitioning from constant model approaches to ELP concepts based on linear regression models significantly improved pIOL power calculations. Linear regression models outperformed constant models, enhancing refractive outcomes for both ICL and IPCL pIOL platforms.

Conclusions: This study underscores the utility of implementing ELP concepts based on linear regression models into pIOL power calculation. Linear regression based ELP models offered substantial advantages for achieving desired refractive outcomes, especially in lower to medium power pIOL models. For pIOL power calculations in both pIOL platforms we tested with preoperative measurements from a Scheimpflug device, we found improved results with the LION 1_{ICL} formula and LION 1_{IPCL} formula. Further research is needed to explore the applicability of these findings to a broader range of pIOL designs and measurement devices.

Introduction:

Phakic posterior chamber intraocular lenses (pIOL) offer an excellent alternative for individuals who are not suitable candidates for corneal laser refractive surgeries due to factors like thin corneas, or extreme refractive errors. Unlike corneal refractive surgeries such as LASIK or PRK, pIOL do not require reshaping the cornea. By avoiding the removal of corneal tissue, the risk of ectasia and postoperative dry eye is minimized.

However, akin to any surgical procedure, pIOL entail their own set of potential difficulties, risks, and complications. While numerous studies have affirmed the effectiveness and safety of these lenses, the importance of the vault, defined as the distance between the anterior lens capsule and the pIOL's posterior surface, is emphasized.[1–5] A vault that falls outside safe ranges elevates the risk of postoperative complications, including pupillary block, cataracts, or pigment dispersion glaucoma.[6]

To mitigate the risk of vault-related complications, various prediction models based on regressions and deep learning have been introduced.[7–9] These models can potentially find utility in pIOL power (pIOLP) calculations, a process that traditionally relies on the manufacturer's calculations. One recent alternative is the LHC formula, which incorporates a thick lens corneal model, permitting the inclusion of corneal thickness and posterior corneal radii into the calculation.[10] In cases where such data is unavailable, the Liou & Brennan model, can be employed.[11] The current variation of the LHC formula introduces an Effective Lens Position (ELP) concept, factoring in anterior chamber depth (ACD) and an effective vault (EV) in the form of an uniform offset constant model, which can be optimized for specific datasets. ELP describes a fictitious position that is usually backcalculated as the value, where the IOL would ideally be located to make the prediction model fit the postoperative refraction. Other factors besides the axial lens position (ALP) and the principle planes also influence ELP.

Meniscus-shaped pIOL are required when the pIOLP is negative. A critical consideration is the position of the principal planes H (object principle plane) and H’ (image principle plane) concerning the anterior lenticular vertex, which switches from the anterior side to the posterior side of the meniscus pIOL when transitioning from positive to negative pIOLP.[12] The concept of the principal plane, as discussed in the previous section, typically applies to optical systems where collimated light rays enter the system . However, the ray vergence at pIOL plane is strictly convergent. Nonetheless, this transition necessitates the use of distinct constants for positively and negatively powered pIOLs, as previously suggested.[10] Additionally, principle-plane positions are intertwined with the ELP. [12] Differences in the relationship between the principal planes and the anterior lenticular surface are observed in low-powered and high-powered meniscus-shaped pIOLs. [12] The lower the (absolute) power of a meniscus lens the more distant is the principal plane from the lens in general. In positive meniscus lenses it moves far in front of the lens if power gets towards zero, and in negative powered meniscus lenses it moves backwards towards infinity if power gets towards zero. Thus, adopting an ELP concept that encompasses the ability to predict the vault and, consequently, the axial lens position (ALP) and the relationship between pIOLP and principal plane position—instead of relying on a uniform constant model — may yield more favorable outcomes.

This study endeavors to address the following questions:

1) Can an ELP algorithm based on a linear regression model, as opposed to a constant model, deliver a more accurate prediction of postoperative refraction?
2) Does including the posterior corneal curvature result in a more accurate prediction of postoperative refraction?

3) Does incorporating the postoperative axial lens position by the means of incorporating the postoperative vault information (to simulate a perfect vault prediction) lead to a more precise prediction of postoperative refraction?
4) Is the concept achieved applicable to various pIOLs?
5) How precise is a vault prediction algorithm ?

Patients and methods

Study design

The data in this study were obtained retrospectively by analyzing the electronic medical records of patients who underwent pIOL implantation at the Eye Center at St. Francis Hospital in Münster, Germany. Two types of pIOLs were used: the implantable phakic contact lens IPCL model 2.0 (IPCL; Caregroup Sight Solution) and the implantable collamer lens V4c (EVO Visian ICL; STAAR Surgical Corporation). The local ethics committee provided a waiver for this study as it exclusively used retrospective patient data already anonymized at the source. The research adheres to the principles outlined in the Declaration of Helsinki. All patients had previously provided written informed consent for the surgical implantation and the potential use of their anonymized data for scientific purposes. The medical records considered for this study encompassed the period from January 2011 to March 2023.

In our previous study, we comprehensively documented the inclusion criteria for the implantation of both pIOL types.[13] Briefly, exclusion criteria included progressive refractive error, an aqueous depth (AQD) of 2.8 mm or less, anterior chamber angle (ACA) less than Grade III as determined by Scheimpflug imaging, insufficient endothelial cell density (ECD) relative to the patient's age, the presence of cataracts, retinal diseases and/or optic neuropathy, ocular inflammation, pregnancy or eastfeeding, the use of hyperopic pIOL, a history of ophthalmic surgery, and postoperative visual acuity lower than 0.3 logMAR. Inclusion criteria were limited to myopic pIOL, complete preoperative biometric and tomographic measurements, and both pre- and postoperative subjective manifest refraction. Preoperative tomography and biometry were conducted using a Scheimpflug device (Pentacam AXL, Oculus, Wetzlar, Germany). The assessment of subjective manifest refraction was performed 3 to 9 months after surgery by one of four experienced optometrists. Refraction was acquired at a refraction lane distance of 6 m using Landolt C optotypes according to DIN/EN/ISO 8596.

Phakic posterior chamber Lens Power Calculation

To determine the target refraction, multiple calculation methods were applied uniformly to all eyes within the datasets. These methods included:

Manufacturer's Calculator: The required pIOLP for the IPCLs was calculated using the manufacturer's IPCL calculator, accessible at http://ipcl1.ipcliol.com/ipcl/. The OCOS software provided by STAAR Surgical and collaborators, accessible at https://evo-ocos.staarag.ch/, was employed to compute the necessary pIOLP for the implanted ICLs. If required, AQD instead of ACD was used for online calculation software.

Finally, various adaptations of the LHC formula were also utilized. The LHC formula is rooted in a corneal thick lens model and offers multiple approaches for calculating pIOLP.

The LHC formula expressed for predicted spectacle refraction Rpost reads:

$$Rpost = \cfrac{1}{\cfrac{1}{\cfrac{1}{\cfrac{1}{\cfrac{1}{\cfrac{1}{\cfrac{1}{\cfrac{1}{\cfrac{1}{\cfrac{1}{\cfrac{Rpre}{1 - Rpre \cdot BVD} + Pca} - \cfrac{CCT}{nc}} + Pcp} - \cfrac{ELP - CCT}{na}} - pIOLP} + \cfrac{ELP - CCT}{na}} - Pcp} + \cfrac{CCT}{nc}} - Pca} + BVD}$$

And after reformulation for the phakic lens power pIOLP it reads:

$$pIOLP = \cfrac{1}{\cfrac{1}{\cfrac{1}{\cfrac{1}{\cfrac{Rpre}{1 - Rpre \cdot BVD} + Pca} - \cfrac{CCT}{nc}} + Pcp} - \cfrac{ELP - CCT}{na}} - \cfrac{1}{\cfrac{1}{\cfrac{1}{\cfrac{1}{\cfrac{Rpost}{1 - Rpost \cdot BVD} + Pca} - \cfrac{CCT}{nc}} + Pcp} - \cfrac{ELP - CCT}{na}}$$

Where the effective lens position ELP and the effective vault EV are expressed by

$$ELP = ACD - EV$$

$$EV = AV + VOC$$

and the vault optimization component VOC reads:

$$VOC = Intercept \cdot VC + ß1 \cdot Predictor\ 1 + ß2 \cdot Predictor\ 2 + ßn \cdot Predictor\ n$$

Rpost= predicted postoperative refraction on spectacle plane; BVD = back vertex spectacle distance; Pcp = posterior corneal power; CCT = central corneal thickness; nc = refractive index of the cornea; na= refractive index of the aqueous; pIOLP = phakic posterior chamber intraocular lens power; Rpre = preoperative refraction; Pca = anterior corneal power; AV = assumed vault; VC = vault coefficient

To calculate pIOLP, an Excel spreadsheet tool was utilized. Several essential input parameters were employed, with units specified as follows: BVD, CCT and ELP in meters (m). Posterior corneal power (Pcp), anterior corneal power (Pca), pIOLP, Rpost and Rpre in diopters (dpt). We used a refractive index of nc=1.376 for the cornea and na=1.336 for the aqueous humour derived from a schematic model eye.[11] Corneal power was calculated with the anterior corneal radius (Rca) and posterior corneal radius (Rcp) as $Pca = \frac{nc-1}{Rca}$and $Pcp = \frac{na-nc}{Rcp}$. Where measurements of CCT and Pcp are not available, the respective data can be derived either from a schematic model eye (e.g. Liou & Brennan)[11] maintaining a fixed ratio of corneal front to back surface curvature, or from biometer/tomograph measurements of the local patient collective at the surgical site. Using the Liou & Brennan model, CCT is set to 500 µm and Rcp is set to $Rcp = \frac{Rca \cdot 6.4}{7.77}$.[11]

IOL Formula Variations:

The study evaluated six variations of the LHC formula for calculating the predicted postoperative refraction. These variations are differentiated by their approach to calculating the VOC, and whether they incorporate standardized or individual posterior curvature measurements. The VC is introduced as a component in formula variations that use a linear regression model VOC. The VC acts as coefficient to the intercept of the linear regression model and can be used to optimize the formula variation (**table 2**).

1. LHC formula with standardized posterior curvature calculated as $Rcp = \frac{Rca \cdot 6.4}{7.77}$. AV is set to 0.004 m and VOC is either
    a. Variation 1a: A simple offset constant model, or
    b. Variation 1b: A multilinear regression model.
2. LHC formula with individual posterior curvature (as measured by the Pentacam). AV is set to 0.004 m and VOC is either
    a. Variation 2a: A simple offset constant model, or
    b. Variation 2b: A multilinear regression model.
3. LHC formula with individual posterior curvature and the postoperatively measured vault as AV, simulating a perfect preoperative prediction of vault magnitude. VOC is either
    a. Variation 3a: A simple offset constant model, or
    b. Variation 3b: A multilinear regression model.

All of these formula variations were tested using data from the ICL dataset, while the IPCL dataset was randomly divided into a training set and a test set to assess the applicability of these calculation concepts to a different pIOL platform.

IOL Formula Optimization:

The IPCL calculator and the OCOS Software could not be optimized.

Every variation of the LHC formula was optimized on the training data and then tested on the test data.

To guide the optimization process, recommendations by Langenbucher et al. for optimization of IOL formulas with one formula coefficient/constant were followed.[14–16] These recommendations emphasized the importance of optimizing lens constants for the specific metric used as the key performance index/marker of success in outcome analysis.[15]

The primary objective was to minimize the mean squared prediction error (MSPE) across all eyes within a dataset. This optimization aimed to achieve the lowest possible MSPE result, indicative of the best refractive outcomes. A minimization of MSPE is equivalent to a root mean squared PE minimization. The optimization process was conducted using the GRG-nonlinear Microsoft Excel Solver function.

By applying Langenbucher et al.'s recommendations and focusing on MSPE minimization, the study sought to fine-tune the VC for each LHC formula variation, ultimately improving the accuracy of refractive predictions.

Vault Prediction

The strategy of the Lens Iterative Optimization Network (LION) vault prediction model is in accordance to the VOC linear regression model. For the manufacturer's vault prediction, we assumed, that all pIOLs were aimed at a postoperative vault of 450 µm.

$$Predicted\ Vault = Intercept \cdot optimizer + ß1 \cdot Predictor\ 1 + ß2 \cdot Predictor\ 2 + ßn \cdot Predictor\ n$$

Surgical technique

Surgery was performed by one experienced surgeon (ST). The surgical procedure and postoperative management were described previously in a detailed manner.[13]

Statistical analysis

For statistical analysis, we utilized Microsoft Excel and SPSS software. We assessed the normal distribution using the Shapiro-Wilk test. Key performance indicators included the MSPE to account for the potential compensation of small prediction errors in phakic eyes through accommodation and the mean absolute prediction error (MAE) as a straightforward and interpretable metric. Consequently, significant attention was given to high prediction errors. The prediction error (PE) refers to the difference of the postoperatively achieved refraction and the predicted refraction. Furthermore, analyses of the PE, absolute PE, and squared PE are presented. We evaluated the percentage of eyes with PE falling within the following limits: ±0.25 dpt,

±0.5 dpt, ±1.00 dpt, and >±1.00 dpt. The same statistics were determined for the vault using limitations of ±50 µm, ±100 µm, ±200 µm, and ±300 µm.

To assess the statistical significance of differences in partly bilateral data for squared PE and absolute PE, we performed generalized linear mixed models, followed by a post-hoc pairwise comparisons using the Wilcoxon signed-rank test. The significance level for this study was set at $p<.05$. Multiple testing correction was applied using the Benjamini-Hochberg procedure.

Results

In this study, a total of 227 eyes from 185 patients were included. The patient cohort comprised 167 eyes from 148 patients who underwent IPCL model 2.0 implantation, and 60 eyes from 35 patients who received an ICL V4c implantation at the study center. The ICL dataset consisted of 60 eyes, involving 35 patients (15 male patients and 20 female patients). Among all pIOL powers, 3.33% had a refractive power equal to or lower than -15 dpt, 46.67% fell between -15 dpt and -10 dpt, and 50.00% were in the range between -10 dpt to -5 dpt. The IPCL training set consisted of 84 eyes, involving 75 patients (27 male and 48 female). Of all pIOL powers, 7.14% had a refractive power equal to or lower than -15 dpt, 50.00% fell between -15 dpt and -10 dpt, and 41.67% were in the range of -10 dpt to -5 dpt. The IPCL test set included 83 eyes from 73 patients (25 male and 48 female). Among all pIOL powers, 7.23% had a refractive power equal to or lower than -15 dpt, 50.60% fell between -15 dpt and -10 dpt, and 39.76% were in the range of -10 dpt to -5 dpt. Demographic data is listed in **Table 1**.

[insert Table 1]

To explore if substituting the offset constant model with a linear regression model leads to a more precise prediction of the postoperative refraction, we used the ICL dataset to establish several formula variations and ELP concepts for the LHC formula, as depicted in **Table 2.**

[insert Table 2]

For LHC variation $1b_{ICL}$, four variables (pIOLP, Rca, ACD, Rpre) improved prediction statistically significantly (*p*<.05). These four variables statistically significantly predicted VOC for an individual PE of 0 ($F(4, 59) = 16.396$, $p<.001$, $R^2=.544$). For LHC variation $2b_{ICL}$, four variables (pIOLP, Rcp, ACD, Rpre) improved prediction statistically significantly (p<.05). These four variables statistically significantly predicted VOC for an individual PE of 0 ($F(4, 59) = 17.118$, $p<.001$, $R^2=.555$). For LHC variation $3b_{ICL}$, four variables (pIOLP, Rcp, ACD, Rpre) improved prediction statistically significantly (*p*<.05). These four variables statistically significantly predicted VOC for an individual PE of 0 ($F(4, 59) = 17.118$, $p<.001$, $R^2=.522$).

[insert table 3]

All formula variations, whether utilizing a constant model or a linear regression model, were employed to assess the impact of including posterior corneal curvature and the ALP (by the means of entering the measured postoperative vault) on predictive accuracy. From the data presented in **Table 3**, it is evident that the inclusion of posterior corneal curvature and postoperative vault measurements did not have a discernible effect on predictive accuracy. This observation held true for formula variations with a constant model as VOC (1a, 2a, 3a) and formula variations that established a multilinear regression model as VOC (1b, 2b, 3b). Notably, no significant differences were observed in squared PE and absolute PE when comparing a-variations with each other or when comparing b-variations with each other. However, b-variations consistently exhibited a trend towards lower MSPE and MAE compared to a-variations. In terms of statistical significance, significant differences in squared PE were observed between each b-variation and the manufacturer's calculation (OCOS) (each $p<.001$), as well as between each b-variation and each a-variation (each $p<.001$). However, no significant differences in squared PE were noted between OCOS and each a-variation. The same was observed for absolute PEs.

Variations 1a and 1b demonstrated improved outcomes and were subsequently employed to evaluate their applicability across another pIOL model.

Using the IPCL training set to establish a VOC linear regression model, we found that for LHC variation $1b_{IPCL}$, four variables (pIOLP, ACD, HCD, Rpre) contributed statistically significantly to the prediction ($p<.05$). These four variables statistically significantly predicted VOC for an individual PE of 0 ($F(4, 83) = 10.006$, $p<.001$, $R^2 = .336$). The derived regression model for LHC variation $1b_{IPCL}$, was established on the IPCL training set. (**Table 2**).

In the IPCL training set, this established variation $1b_{IPCL}$ performed statistically significantly better (regarding squared PE and absolute PE) than variation $1a_{IPCL}$ and the IPCL calculator. There was no significant difference between variation $1a_{IPCL}$ and the IPCL calculator (**Table 4**).

[insert Table 4]

When examining the performance of various variations on the IPCL test set (as depicted in **Table 4**), several important trends and findings emerge: Variation $1b_{IPCL}$, derived from the IPCL training set, and the optimized Variation $1b_{ICL}$, derived from the ICL dataset, consistently exhibited a trend toward achieving the lowest MSPE and MAE. Both achieved a significantly lower squared PE and absolute PE compared to either, the manufacturer's IPCL calculator software or Variation $1a_{ICL}$. Before optimization, Variation $1b_{ICL}$ resulted in a lower MSPE and MAE than the IPCL calculator, but there were no significant differences when testing squared PE and absolute PE.

Shifting the focus to testing the generalizability of results from the IPCL training set to other pIOL platforms using the ICL dataset, the following key observations were made from **table 4**: The OCOS software yielded a significantly higher squared PE and absolute PE than either, Variation $1b_{ICL}$, Variation $1b_{IPCL}$, and the optimized Variation $1b_{IPCL}$. All three performed statistically superior compared to Variation $1a_{IPCL}$. Variation $1b_{ICL}$ achieved significantly better results compared to Variation $1a_{ICL}$.

Figure 1 displays trend errors of pIOLP (**Figure 1a**), Rpre (**Figure 1b**) and ACD (**Figure 1c**) against PE in the IPCL test set. We can read out of the figures, that the slope of each trend error gets considerably flatter and/or offsets become smaller for Variation $1b_{ICL}$ and optimized Variation $1b_{IPCL}$.

[insert Figure 1]

Finally, using the postOP vault in order to describe the ALP requires a high predictability of ALP and, consequently, the vault. Variation $3b_{ICL}$ simulates a perfect vault prediction. Similar to developing a linear regression model for VOC, we created a linear regression model for the postoperative vault. Therefore, we assessed the utility of age, pIOL size, Rpre, the horizontal and vertical vector components of refractive astigmatism J_0 and J_{45}[17], ACD, Rca, Rcp, CCT, HCD, pIOLP as predictors for the vault and pIOL sizing in the IPCL training set. We then applied this model to both the IPCL test set and the ICL set. In the IPCL training set, three variables (ACD, HCD, and pIOL size) were found to contribute significantly to the prediction ($p<.05$). These three variables collectively had a statistically significant effect on predicting postoperative vault outcomes ($F(3, 83) = 15.325$, $p<.001$, $R^2=.365$). To enhance the accuracy of vault prediction within a dataset, an optimizer coefficient was introduced to the intercept of the regression. This led to the formulation of the LION vault prediction equation:

$$LION\ Vault(IPCL) = 210.406 \cdot optimizer + 345.804 \cdot ACD - 186.426 \cdot HCD + 95.335 \cdot pIOL\ size$$

When examining the performance of our prediction model on the IPCL dataset, we can read out from **table 5**, that the LION Vault Prediction $_{(IPCL)}$ showed a lower trend for MAE and MSE than the IPCL Calculator prediction (assuming that the software aims at a vault of 450 µm in each case). Differences in squared PE and absolute PE were statistically significant.

Shifting the focus to testing the generalizability of results in the ICL testing set, following key observations were made from **table 5**: The LION Vault Prediction$_{(IPCL)}$ after optimization showed a trend towards similar MAE and MSE than the manufacturer's OCOS software. Both performed with a tendency towards a lower MSE and MAE than the LION Vault Prediction$_{(IPCL)}$ before optimization. The optimized version achieved significantly lower squared and absolute PEs compared to the LION Vault Prediction$_{(IPCL)}$ before optimization.

[insert table 5]

Discussion:

In order to meet the patient's expectations a low postoperative refractive error needs to be achieved and refractive surprises need to be avoided.[18] To achieve a desired refractive outcome the meticulous lens power calculation is as important as a precise surgical technique.[18] **Table 6** depicts the effects of various parameters on pIOLP calculation in myopic eyes.

[insert Table 6]

Moreover, the difference between the postoperative phakic ALP and the preoperative expected position influences the refractive outcome as well. [19,20] For non-empirical pIOL power calculation approaches based on physical optics, the postoperative pIOL position needs to be anticipated prior to the operation. The vault is typically predicted within a range between 250 µm and 750 µm.[20,21] Serra et al. evaluated an association between the postoperative spherical equivalent and the vault of the pIOL with the help of paraxial optics.[21] For a negative power pIOL, an underestimation of the vault results in hyperopic refraction, while an overestimation of the vault leads to myopic refraction.[21] This matches with the findings of Kamiya et al., who described a trend to postoperative hyperopia in eyes with a higher vault in 75 evaluated eyes, but the effect was not statistically significant.[22] The effect of the vault is greater in cases with a vault outside of the optimal range and in pIOL with a higher lens power, which may be attributed to further factors than just pIOL position. [21]

One of our study goals was to explore the utility of a vault/ALP prediction in an ELP algorithm for pIOL power calculation. In order to fully judge the maximum potential, we did not implement our own vault prediction model, but rather incorporated the postoperatively measured vault as a placeholder for the best possible prediction algorithm of the postoperative vault and in turn the ALP. We therefore explored the effect of a perfect vault prediction. Overall, we were unable to find a benefit after incorporating the measured postoperative vault into pIOL calculations (**Table 3**). In the ICL dataset, differences between ELP concepts based on a simple constant model using a fixed vault of 0.4mm (variations $1a_{ICL}$ and $2a_{ICL}$) and the postoperative vault (variation $3a_{ICL}$) were miniscule. Similarly, there were only slight differences between prediction models, when using an ELP concept with a linear regression model instead of a constant model between variations that did incorporate the postoperative vault (variation $3b_{ICL}$) and those that did not (variations $1b_{ICL}$ and $2b_{ICL}$). Hence, we were unable to establish the utility of a vault prediction concept in the calculation of pIOLs with a thin lens pIOL model. Furthermore, our vault prediction model still had approximately 17% of predictions deviating by more than 200 µm and about 7% deviating by more than 300 µm, which could negatively impact results compared to incorporating the measured vault. Making use of the RCP (variations 2 a and b) instead of a fixed ratio of anterior and posterior curvature (variations 1 a and b) did not have a significant effect on results (**table 3**).

In addition to evaluating the postoperative vault and Rcp for power calculations, we also explored the possibility of enhancing pIOL power calculations by transitioning from the traditional effective vault concept, which relies on a simple constant model, to an ELP concept (variations from category a) based on a linear regression model (variations from category b). **Table 3** provides direct evidence that all linear regression model concepts outperformed the constant model concepts significantly. To avoid overfitting, we then focused exclusively on variations 1a and 1b. Variations 2a and 2b do show potential utility, particularly in pIOL calculations involving altered corneas, as seen in conditions such as keratoconus or corneal scarring. However, considering that Rcp may exhibit systematic differences between devices or, especially when using Scheimpflug technology, may be sensitive to corneal opacifications such as haze or scarring, we found variations 1a and 1b to be effective and suitable for normal cases. [23,24] The transition to a linear regression model demonstrated its generalizability, as evidenced by lower MSE and MAE in both the ICL dataset and the IPCL training and test sets (as shown in **Tables 3 and 5**). This approach proved highly successful, with significantly reduced squared PE and absolute PE observed when using formula variations with this linear regression model in the test set, in comparison to the manufacturer's calculations. This held true for both pIOLs, the ICL, and the IPCL.

It's interesting to note that both linear regression models, developed independently from each other in the IPCL training set and the ICL dataset, appeared to be beneficial not only for their respective pIOL platforms but also for the other pIOL platform (as demonstrated in **Tables 3 and 4**). We think that formula variations using a constant model (variation 1a) benefit from an optimization of the VOC before they can be applied to another pIOL platform. In contrast, variations based on a linear regression model (variation 1b) can be used without optimization. However, optimizing the VC does result in slightly flatter trend error slopes (as shown in **Figure 1**) and slightly lower MSPE and MAE values (as presented in **Table 4**). For now, we recommend using the IPCL-derived linear regression model (Variation $1b_{IPCL}$) for IPCLs and the ICL-derived linear regression model (Variation $1b_{ICL}$) for ICLs. This recommendation stands until further studies on larger datasets can confirm these results. As previously explained, hyperopic pIOLs require a different regression model and should not be calculated using any concepts derived from this study before undergoing a validation study. To differentiate between formula versions more clearly, we have decided to name formula variations with a linear regression model (Variations 1b/2b/3b) as LION 1/2/3 formulas and maintain the use of LHC formula for formula variations with a constant model (Variations 1a/2a/3a). Following cross-validation, it's customary to incorporate all available eyes from the training and test sets into an overall regression model. The linear regression models for the LION 1 formula for all available ICLs and IPCLs were:

LION 1_{ICL}

$$VOC = -3.772 \cdot VC - 1.044 \cdot pIOLP + 1.026 \cdot Rpre + 0.734 \cdot Rca - 0.813 \cdot ACD$$

LION 1_{IPCL}

$$VOC = -3.169 \cdot VC - 1.155 \cdot pIOLP + 1.174 \cdot Rpre + 0.695 \cdot Rca - 0.757 \cdot ACD$$

IOLP, Rpre, RCA, HCD, and ACD were identified as significant contributors to the linear regression model. It's important to note that HCD may pose a risk of overfitting, given the well-established variations in HCD measurements among different devices, which can limit their interchangeability. [25,26] The instrument used to measure segment dimensions may be a cause for overfit in further aspects of our linear regression model. We observed systematic differences in ACD between two modern biometers (IOLMaster 700, Carl Zeiss Meditec AG, and Anterion, Heidelberg Engineering). [27,28] Anecdotally, we also observed systematic differences in ACD and HCD between IOLM500 and MS-39 (currently unpublished data). Unfortunately, we were unable to explore the utility of AL and newly established parameters such as the angle-to-angle, spur-to-spur, and sulcus-to-sulcus distance and depth, or crystalline lens rise for the regression model. This limitation arises because these parameters require different instruments beyond the capabilities of the Pentacam.

The results obtained with the ICL in this study were quite similar to our previously published findings with ICL when biometry was conducted using the IOLM700.[10] However, it's worth noting that, although refractive results showed similarities, we observed a notable difference in the ELP compared to our recent study. In our previous publication, the ELP of the ICL dataset was located more posteriorly to the pIOL, whereas in this study, the ELP of the ICL dataset appears to be more anteriorly to the pIOL. [10] When optimized for the smallest MAE rather than MSPE, the VOC for variation 1a changes from -0.411 to -0.350. If optimized for mean PE of 0, it changes to -0.385. From a physical optics standpoint, it makes sense for the ELP position to be posterior to the pIOL in high-power minus meniscus pIOLs since the principal plane H is located behind the back vertex. The primary difference in both datasets is the measurement instrument, as the Pentacam was used in this study. Moreover, the SD of the PE was higher than in our previous research. Our results appear consistent for both pIOL platforms in this study. Further data on IOL geometry may offer opportunities to enhance predictive accuracy even further.[29–31] Complications and rotation rates for our dataset have been previously described in previous studies.[13,32]

Our vault prediction model (LION Vault Prediction$_{(IPCL)}$) yielded positive results within the same pIOL platform **(table 5)**. After optimization, it demonstrated performance similar to the manufacturer's calculation in the ICL dataset, assuming that the manufacturer targeted a vault of 450 µm in each case. This observation hints at the possibility that sizing nomograms developed for one pIOL platform may not readily translate to another. Our nomogram is based on Pentacam data, and we are uncertain about its applicability to different devices, as discussed in the previous two paragraphs. In the case of different devices, additional coefficients, such as HCD, can be incorporated into the predictor variables. In line with our linear regression model for refractive prediction, we've introduced a single optimizer coefficient in the iteration of the linear regression model for vault prediction. This allows clinicians to fine-tune the vault algorithm to suit their specific clinic and devices. However, we advise preliminary testing on small cohorts before integrating it into a standardized surgical algorithm. This caution is necessary because our study primarily focused on cross-validating the IPCL and Pentacam algorithm and didn't explore results after optimizing for another pIOL or measurement device. We are committed to refining all our models, including those for ICL and IPCL, other pIOLs, both refractive and vault predictions, and across various devices such as Pentacam and IOLMaster, as new datasets become available in the future. Following cross-validation, it's customary to incorporate all available eyes from the training and test sets into an overall regression model. The linear regression model for the LION Vault Prediction$_{(IPCL)}$ formula for all available IPCL was:

$$\text{LION Vault Prediction}_{(IPCL)} = 356.760 * optimizer + 4.326 * pIOL\ Size + 323.444 * ACD - 92.938 * HCD$$

Limitations of the study include small cohorts for specific pIOL designs and the preoperative use of only Scheimpflug measurement, which may differ when other devices are used. The amount of high powered pIOL was rather low in the dataset and the sample size was too low for a separate statistical analysis of the training and test dataset. The applicability of our LION formula variations 1/2/3 should be examined in further research. The measured postoperative vault simulates results from a perfect vault prediction. Real world results with a vault prediction concept may suffer if the prediction accuracy of the postoperative vault is less than optimal. All measurements were performed 3 to 9 months after surgery. Changes of the vault or refraction over time were not part of this paper, but should be analyzed in future studies.

In summary, this study sheds light on the significance of considering the ALP by means of the postoperative vault in pIOL power calculations and demonstrates the potential benefits of using an ELP concept based on a linear regression model for improved refractive outcomes. Especially the latter seems to be beneficial and leads to better outcomes than the manufacturer-based prediction in both pIOL platforms.

Hence, for low and medium powered pIOL models used in this study (IPCL and ICL) with preoperative measurement obtained with the Pentacam, we recommend power calculation with the LION 1_{ICL} formula and LION 1_{IPCL} formula (formula variation $1b_{ICL}$ and variation $1b_{IPCL}$). Adding the ALP/vault prediction or posterior corneal curvature to the concept does not seem to be beneficial compared to this formula variation, at least in normal eyes with unaltered corneas. The main problem of all meniscus lenses is that the principal plane is always outside the lens geometry. In a very low powered lens it could be 1 cm in front or behind the pIOL. Measurement of the equivalent power on the optical bench is not possible without design data as we do not know the reference plane. If the exact shape of the pIOL for all power steps is available, the exact location of H could be derived. And the location of this H should be studied instead of the posterior pIOL vertex if we use a thin lens model for the pIOL.

References

1. Choi JH, Lim DH, Nam SW, Yang CM, Chung ES, Chung T-Y. Ten-year clinical outcomes after implantation of a posterior chamber phakic intraocular lens for myopia. J cat refract surg 2019;45(11):1555-1561.
2. Montés-Micó R, Ruiz-Mesa R, Rodríguez-Prats JL, Tañá-Rivero P. Posterior-chamber phakic implantable collamer lenses with a central port: a review. Acta ophthalmol 2021;99(3):e288-e301.
3. Moya T, Javaloy J, Montés-Micó R, Beltrán J, Muñoz G, Montalbán R. Implantable Collamer Lens for Myopia: Assessment 12 Years After Implantation. J refract surg (Thorofare, N.J. : 1995) 2015;31(8):548-556.

4. Sanders DR, Doney K, Poco M. United States Food and Drug Administration clinical trial of the Implantable Collamer Lens (ICL) for moderate to high myopia: three-year follow-up. Ophthalmol 2004;111(9):1683-1692.
5. Sanders DR, Vukich JA, Doney K, Gaston M, Implantable Contact Lens in Treatment of Myopia Study Group. U.S. Food and Drug Administration clinical trial of the Implantable Contact Lens for moderate to high myopia. Ophthalmol 2003;110(2):255-266.
6. Packer M. Meta-analysis and review: effectiveness, safety, and central port design of the intraocular collamer lens. Clin ophthalmol (Auckland, N.Z.) 2016;10:1059-1077.
7. Kamiya K, Ryu IH, Yoo TK, et al. Prediction of Phakic Intraocular Lens Vault Using Machine Learning of Anterior Segment Optical Coherence Tomography Metrics. Am J Ophthalmol 2021;226:90-99.
8. Shen Y, Wang L, Jian W, et al. Big-data and artificial-intelligence-assisted vault prediction and EVO-ICL size selection for myopia correction. Br J Ophthalmol 2023;107(2):201-206.
9. Reinstein DZ, Lovisolo CF, Archer TJ, Gobbe M. Comparison of postoperative vault height predictability using white-to-white or sulcus diameter-based sizing for the visian implantable collamer lens. J refract surg (Thorofare, N.J. : 1995) 2013;29(1):30-35.
10. Wendelstein JA, Hinterberger S, Hoffmann PC, et al. Evaluation of phakic intraocular lens power calculation using the new Linz-Homburg-Castrop formula and comparison with four conventional methods. J cat refract surg 2023;49(2):119-125.
11. Liou HL, Brennan NA. Anatomically accurate, finite model eye for optical modeling. J Opt im sci vis 1997;14(8):1684-1695.

12. Haigis W. Intraocular lens calculation in extreme myopia. J cat refract surg 2009;35(5):906-911.

13. Taneri S, Dick HB. Initial clinical outcomes of two different phakic posterior chamber IOLs for the correction of myopia and myopic astigmatism. Grae arch clin exp ophthalmol 2022;260(5):1763-1772.

14. Langenbucher A, Szentmáry N, Cayless A, Wendelstein J, Hoffmann P. Strategies for formula constant optimisation for intraocular lens power calculation. PloS one 2022;17(5):e0267352.

15. Langenbucher A, Szentmáry N, Cayless A, et al. IOL formula constants - strategies for optimization and defining standards for presenting data. Ophthalm research 2021.

16. Langenbucher A, Schwemm M, Eppig T, Schröder S, Cayless A, Szentmáry N. Optimal Dataset Sizes for Constant Optimization in Published Theoretical Optical Formulae. Cur Eye Res 2021:null-null.

17. Holladay JT, Moran JR, Kezirian GM. Analysis of aggregate surgically induced refractive change, prediction error, and intraocular astigmatism. J cat refract surg 2001;27(1):61-79.

18. Lovisolo CF, Reinstein DZ. Phakic intraocular lenses. Sur ophthalmol 2005;50(6):549-587.

19. Nawa Y, Ueda T, Nakatsuka M, et al. Accommodation obtained per 1.0 mm forward movement of a posterior chamber intraocular lens. J cat refract surg 2003;29(11):2069-2072.

20. Holladay JT. Refractive Power Calculations for Intraocular Lenses in the Phakic Eye. Am J Ophthalmol 1993;116(1):63-66.

21. Serra P, Sánchez Trancón Á, Torrado Sierra O, Baptista A, Cerpa Manito S. Posterior Chamber Phakic Intraocular Lenses for the Correction of Myopia: Factors Influencing the Postoperative Refraction. Optics 2021;2(4):292-305.
22. Kamiya K, Shimizu K, Kawamorita T. Changes in vaulting and the effect on refraction after phakic posterior chamber intraocular lens implantation. Journal of cat refract surg 2009;35(9):1582-1586.
23. Mendes Baiao T, Wendelstein J, Seiler TG. Comparison of Corneal Thickness Measurements After Customized Corneal Crosslinking Using High-Resolution Optical Coherence Tomography and Scheimpflug Tomography. Cornea 2023;42(9):1104-1109.
24. Wendelstein JA, Reifeltshammer SA, Cooke DL, et al. The 10,000 Eyes Study: Analysis of Keratometry, Abulafia-Koch regression transformation, and Biometric Eye Parameters Obtained With Swept-Source Optical Coherence Tomography. Am J Ophthalmol 2023;245:44-60.
25. Tañá-Rivero P, Aguilar-Córcoles S, Rodríguez-Prats JL, Montés-Micó R, Ruiz-Mesa R. Agreement of white-to-white measurements with swept-source OCT, Scheimpflug and color LED devices. Int Ophthalmol 2021;41(1):57-65.
26. Buckenham Boyle A, Namkung S, Shew W, Gokul A, McGhee CNJ, Ziaei M. Repeatability and agreement of white-to-white measurements between slit-scanning tomography, infrared biometry, dual rotating Scheimpflug camera/Placido disc tomography, and swept source anterior segment optical coherence tomography. PloS one 2021;16(7):e0254832.
27. Lender R, Mirsky D, Greenberger R, et al. Evaluation of three biometric devices: ocular parameters and calculated intraocular lens power. Scientific reports 2022;12(1):19478.

28. Langenbucher A, Szentmáry N, Cayless A, Wendelstein J, Hoffmann P. Comparison of 2 modern swept-source optical biometers-IOLMaster 700 and Anterion. Grae arch clin exp ophthalmol 2023;261(4):999-1010.
29. Olsen T, Cooke DL, Findl O, et al. Surgeons need to know more about intraocular lens design for accurate power calculation. J cat refract surg 2023;49(6):556-557.
30. Langenbucher A, Szentmáry N, Cayless A, et al. Monte-Carlo simulation of a thick lens IOL power calculation. Acta ophthalmol 2023.
31. Langenbucher A, Hoffmann P, Cayless A, et al. Considerations of a thick lens formula for intraocular lens power calculation. Z med Phys 2022.
32. Kilic D, Förster A, Mertens E, Dick HB, Taneri S. Rotational Stability After Implantation of Two Different Phakic Toric Intraocular Lenses. J refract surg (Thorofare, N.J. : 1995) 2023;39(7):463-472.

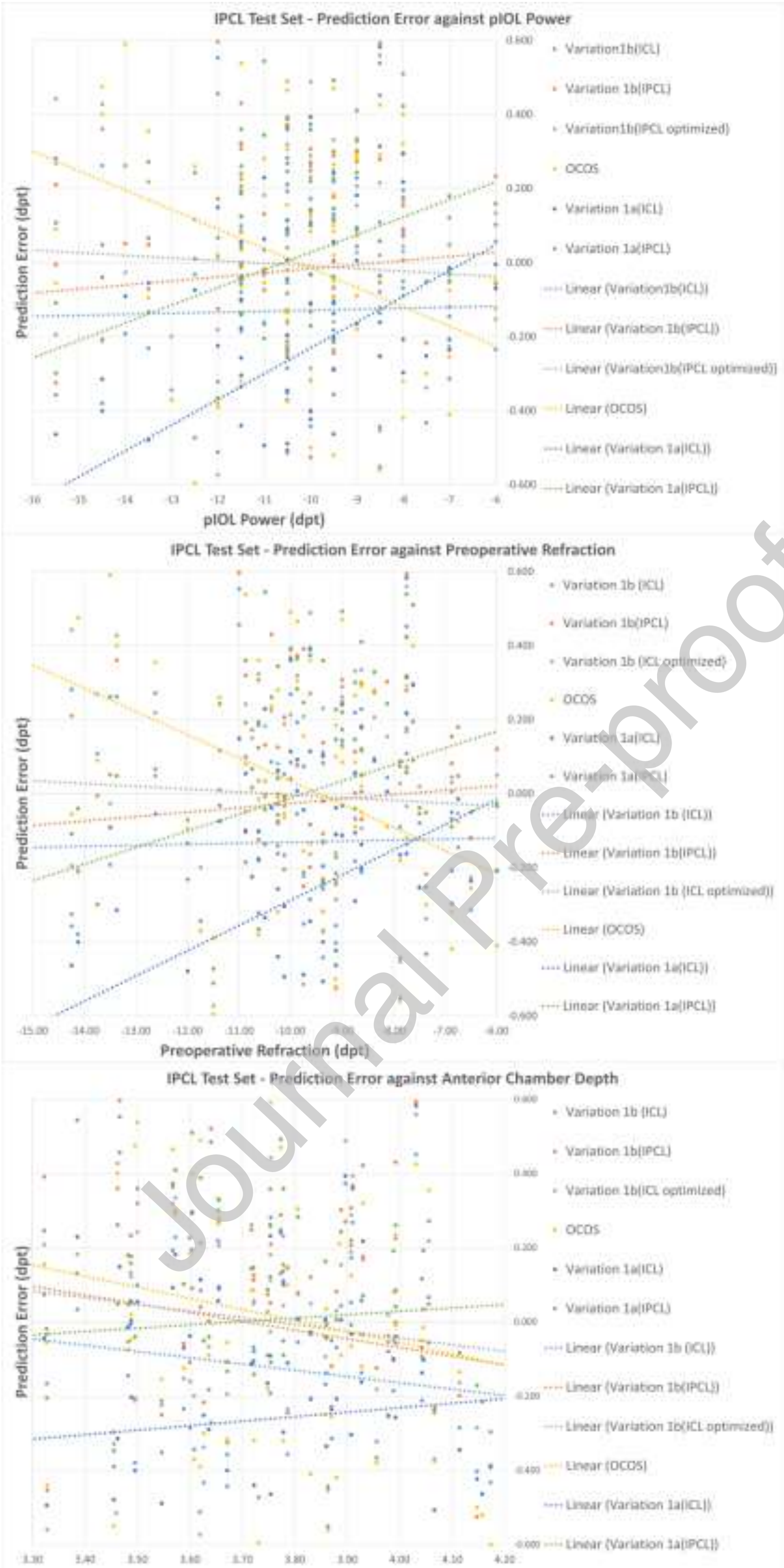

Figure 1: Trend errors characterized by the formula prediction error as a function of the phakic posterior chamber intraocular lens power (Figure 1a), preoperative

refraction (Figure 1b), and anterior chamber depth Figure 1c). The IPCL test set is exemplarily displayed.

		mean	SD	Med	IQR	95% CI upper	95% CI lower
Age (years)	ICL Set	36.75	10.01	38.50	19.00	51.00	18.00
	IPCL Training Set	33.62	8.20	32.00	13.00	46.00	21.08
	IPCL Test Set	32.58	7.63	32.00	12.00	44.00	21.00
Follow up time (months)	ICL Set	3.48	0.99	3.00	1.00	6.00	2.00
	IPCL Training Set	3.21	1.05	3.00	1.00	6.00	2.00
	IPCL Test Set	3.03	0.98	3.00	1.00	6.00	2.00
Preoperative SEQ (dpt)	ICL Set	-9.35	2.45	-9.13	3.03	-5.63	-14.54
	IPCL Training Set	-9.51	2.57	-9.50	3.00	-5.06	-16.09
	IPCL Test Set	-9.89	3.50	-9.69	3.19	-4.43	-20.08
ACD (mm)	ICL Set	3.84	0.34	3.77	0.54	4.51	3.37
	IPCL Training Set	3.80	0.28	3.76	0.43	4.37	3.33
	IPCL Test Set	3.83	0.29	3.80	0.43	4.37	3.30
Rmean (mm)	ICL Set	7.69	0.24	7.70	0.37	8.16	7.30
	IPCL Training Set	7.64	0.27	7.61	0.30	8.20	7.14
	IPCL Test Set	7.66	0.25	7.63	0.28	8.18	7.20

Table 1: Demographic data. Displayed is age, preoperative refraction (SEQ = spherical equivalent), anterior chamber depth (ACD), and mean anterior corneal curvature (Rmean).
SD = standard deviation; med = median; IQR = interquartile range; 95%CI = 95% confidence interval

ICL dataset	
LHC variation $1b_{ICL}$	$VOC = -3.772 \cdot VC - 1.044 \cdot pIOLP + 1.026 \cdot Rpre + 0.734 \cdot Rca - 0.813 \cdot ACD$
LHC variation $2b_{ICL}$	$VOC = -3.905 \cdot VC - 1.104 \cdot pIOLP + 1.068 \cdot Rpre + 0.840 \cdot Rcp - 0.757 \cdot ACD$
LHC variation $3b_{ICL}$	$VOC = -3.871 \cdot VC - 1.104 \cdot pIOLP + 1.068 \cdot Rpre + 0.840 \cdot Rcp - 0.757 \cdot ACD$
IPCL training set	
LHC variation $1b_{IPCL}$	$VOC = -1.983 \cdot VC - 1.095 \cdot IOLP - 1.218 \cdot ACD + 1.110 \cdot Rpre + 0.500 \cdot HCD$

Table 2: Multilinear regression models to predict the perfect vault optimizing component (VOC) for each of the LHC formula variations (1b, 2b and 3b). Multiple predictors were tested, including age, phakic posterior chamber intraocular lens power (pIOLP), phakic posterior chamber intraocular lens sizing, preoperative refraction (Rpre), mean anterior corneal radius (Rca), anterior chamber depth (ACD), mean posterior corneal radius (Rcp), central corneal thickness, and horizontal corneal diameter (HCD).
VC= vault coefficient.

Method	VC/VOC	MAE	MSPE	mPE	medPE	SDPE	95% CI AE	±0.25 dpt	±0.50 dpt	±0.75 dpt	±1 dpt
variation $3b_{ICL}$	0.990	0.237	**0.088**	0.000	-0.040	0.299	0.020 – 0.630	61.67	88.33	100	100
Variation $2b_{ICL}$	1.002	0.232	**0.091**	0.003	-0.010	0.305	0.002 – 0.603	63.33	90.00	98.33	100
Variation $1b_{ICL}$	1.002	0.240	**0.093**	0.003	-0.011	0.308	0.022 – 0.617	60	88.33	98.33	100
variation $3a_{ICL}$	-0.378	0.345	**0.189**	-0.013	-0.047	0.439	0.036 – 0.866	50.00	68.33	95.00	98.33
variation $2a_{ICL}$	-0.412	0.345	**0.189**	-0.013	-0.047	0.439	0.036 – 0.866	50.00	68.33	95.00	98.33
Variation $1a_{ICL}$	-0.411	0.346	**0.189**	-0.014	-0.049	0.439	0.042 – 0.866	50	68.33	95.00	98.33
OCOS Software	n/a	0.347	**0.200**	0.182	0.170	0.412	0.015 – 1.086	41.67	78.33	91.67	95.00

Table 3 shows refractive results of all formula variations. All variations showed a trend towards a lower mean squared and mean absolute prediction error (MSPE and MAE) than the manufacturer calculation (OCOS software). Generally, all variations that used a multilinear regression model for the vault optimizing component (VOC) (b-variations) showed a trend towards lower MSPE and MAE than variations that used a constant model for VOC (a-variations). Posterior corneal curvature (Pcp) and vault magnitude had little to no effects on PSME and MAE. Formulae are ranked by MSPE.
Variation 1b: Characteristics: Linear regression model; Pcp: Not included; Vault: Not included.
Variation 2b: Characteristics: Linear regression model; Pcp: Included; Vault: Not included.
Variation 3b: Characteristics: Linear regression model; Pcp: Included; Vault: Included.
Variation 1a: Characteristics: Offset constant model; Pcp: Not included; Vault: Not included.
Variation 2a: Characteristics: Offset constant model; Pcp: Included; Vault: Not included.
Variation 3a: Characteristics: Offset constant model; Pcp: Included; Vault: Included.

VC/VOC: vault coefficient/vault optimizing component; MAE = mean absolute prediction error ; MSPE = mean squared prediction error, mPE = mean prediction error; medPE = median prediction error; SDPE = standard deviation of prediction error; 95%CI AE = 95% confidence interval of the absolute prediction error; ±X dpt = percentage of eyes within an absolute prediction error of X diopters.

Method	VC/VOC	MAE	MSPE	mPE	medPE	SDPE	95% CI AE	±0.25 dpt	±0.50 dpt	±0.75 dpt	±1 dpt
					IPCL Training set						
Variation $1b_{IPCL}$	1.000	0.256	**0.107**	0.007	0.030	0.329	0.013 – 0.716	58.33	84.52	97.62	98.81
Variation $1a_{IPCL}$	0.092	0.323	**0.180**	0.033	0.014	0.426	0.009 – 0.872	47.62	80.95	91.67	97.62
IPCL calculator	n/a	0.338	**0.182**	0.028	0.038	0.428	0.027 – 0.988	46.43	77.38	91.76	97.62
					IPCL Test Set						
Variation $1b_{ICL}$ optimiert	0.940	0.262	**0.114**	-0.007	0.030	0.339	0.027 – 0.768	62.65	84.34	96.39	100
Variation $1b_{ICL}$	1.002	0.271	**0.130**	-0.130	-0.080	0.338	0.032 – 0.852	59.04	86.75	91.57	97.59
Variation $1b_{IPCL}$	1.000	0.269	**0.133**	-0.021	0.040	0.366	0.006 – 0.867	56.63	83.13	96.39	98.80
Variation $1a_{IPCL}$	0.092	0.309	**0.170**	0.010	0.082	0.415	0.027 – 0.279	53.01	81.93	92.77	97.59
IPCL calculator	n/a	0.336	**0.186**	0.005	-0.10	0.434	0.020 – 1.228	39.76	79.52	95.18	96.39
Variation $1a_{ICL}$	-0.411	0.352	**0.257**	-0.256	-0.176	0.440	0.006 – 1.225	51.81	80.72	86.75	93.98
					ICL Set						
Variation $1b_{ICL}$	1.002	0.240	**0.093**	0.003	-0.011	0.308	0.022 – 0.617	60.00	88.33	98.33	100
Variation $1b_{IPCL}$ (optimized VC)	1.081	0.259	**0.122**	0.020	-0.20	0.351	0.012 – 0.776	58.33	85.00	96.67	98.33
Variation $1b_{IPCL}$	1.000	0.266	**0.129**	0.103	0.060	0.347	0.027 – 0.751	60.00	85.00	96.67	98.33
Variation $1a_{ICL}$	-0.411	0.346	**0.189**	-0.014	-0.049	0.439	0.042 – 0.866	50.00	68.33	95.00	98.33
OCOS Software	n/a	0.347	**0.200**	0.182	0.170	0.412	0.015 – 1.086	41.67	78.33	91.67	95.00
Variation $1a_{IPCL}$	0.092	0.404	**0.258**	0.244	0.229	0.450	0.004 – 1.055	35.00	71.67	83.33	95.00

Table 4 shows refractive results of all formula variations. All variations showed a trend towards a lower mean squared and mean absolute prediction error (MSPE and MAE) than the manufacturer calculation (OCOS software). Generally, all variations that used a multilinear regression model for the vault optimizing component (VOC) (b-variations) showed a trend towards lower MSPE and MAE than variations that used a constant model for VOC (a-variations). Posterior corneal curvature and vault magnitude had little to no effects on MSPE and MAE. Formulae are ranked by MSPE.
Variation 1b: Characteristics: Linear regression model; PCP: Not included; Vault: Not included.
Variation 1a: Characteristics: Offset constant model; PCP: Not included; Vault: Not included.

VC/VOC: vault coefficient/vault optimizing component; MAE = mean absolute prediction error ; MSPE = mean squared prediction error, mPE = mean prediction error; medPE = median prediction error; SDPE = standard deviation of prediction error; 95%CI AE = 95% confidence interval of the absolute prediction error; ±X dpt = percentage of eyes within an absolute prediction error of X diopters.

Method	Optimizer	MAE	MSPE	mPE	medPE	SDPE	95% CI AE	±50 µm	±100 µm	±200 µm	±300 µm
					IPCL Training set						
Vault $prediction_{(IPCL)}$	1.002	110.92	**19331.66**	0.00	5.33	139.87	7.30 – 320.40	28.57	51.19	85.71	96.43
IPCL calculator	n/a	160.58	**41095.20**	103.08	117.50	175.60	0.00 – 462.25	23.81	33.33	69.05	86.90

IPCL Test Set											
Vault prediction$_{(IPCL)}$ optimized	1.045	126.63	**33428.87**	0.00	-18.78	183.95	6.14 – 397.29	31.33	51.81	83.13	92.77
Vault prediction$_{(IPCL)}$	1	125.97	**33517.60**	9.42	-9.36	183.95	5.43 – 405.77	28.92	54.22	80.72	92.77
IPCL calculator	n/a	147.55	**35872.37**	103.46	89.00	159.61	6.0 – 389.80	24.10	44.58	71.08	89.16
ICL Set											
Vault prediction$_{(IPCL)}$ optimized	0.567	173.17	**58046.16**	0.00	-46.04	242.96	16.03 – 624.64	18.33	45.00	68.33	86.67
OCOS	n/a	179.62	**58363.65**	38.05	0.00	240.58	0.00 – 588.13	25.00	36.67	61.67	83.33
Vault prediction$_{(IPCL)}$	1	203.52	**66377.78**	-91.28	-137.32	242.96	2.31 – 551.36	16.67	26.67	56.67	75.00

Table 5 shows results of LION vault prediction in the ICL dataset, the IPCL training set, and the IPCL test set.

MAE = mean absolute prediction error ; MSPE = mean squared prediction error, mPE = mean prediction error; medPE = median prediction error; SDPE = standard deviation of prediction error; 95%CI AE = 95% confidence interval of the absolute prediction error; ±X µm = percentage of eyes within an absolute prediction error of X µm.

Rpre (dpt)	-5	-10	-17
ACD (mm)	3.70	3.15	3.33
R / K (mm / dpt)	8.29/40.71	7.57/44.58	7.56 /44.64
Formula variation	1a	1a	1a
ELP (mm)	2.91	2.36	2.54
Emmetropizing pIOLP (dpt)	-5.61	-10.24	-16.37
ΔP/ΔACD	-0.33 dpt/1 mm	-1.07 dpt/1 mm	-0.92 dpt/1 mm
ΔP/ΔR	0.15 dpt/1 mm	0.27 dpt/1 mm	0.46 dpt/1 mm
ΔP/ΔK	-0.01 dpt/1 dpt	-0.02 dpt/1 dpt	-0.03 dpt/1 dpt
ΔP/ΔELP	-0.33 dpt/1 mm	-0.62 dpt/1 mm	-0.92 dpt/1 mm

Table 6 depicts three fictional example eyes to illustrate the effects of different influencing parameters on emmetropization and phakic posterior chamber intraocular lens power using variation 1a with vault optimization component of -0.411.
Rpre = preoperative refraction, ACD = anterior chamber depth, R = radius of corneal curvature, K = Keratometric power of the cornea, ELP = effective lens position, pIOLP = phakic posterior chamber intraocular lens power

Jascha Wendelstein specializes in intraocular lens (IOL) calculations, designs, and combinability. His expertise extends to corneal and refractive surgery. With a keen interest in anterior segment diagnostics, including biometry, tomography, and AS-OCT, he is dedicated to advancing precision in refractive surgery and eye care.

Declarations of interest:

Dr. Wendelstein reports research support from Carl Zeiss Meditec AG. He reports personal fees from Carl Zeiss Meditec AG, Alcon Surgical, Rayner Surgical, and Johnson & Johnson Vision outside of the submitted work. He was supported by an “ESCRS Peter Barry Fellowship Award”.

Dr. Langenbucher reports personal fees from Hoya Surgical and Johnson & Johnson Vision outside the submitted work.

Dr. Seiler reports personal fees and consultant functions from Glaucos, Schwind and Ziemer outside of the submitted work.

Dr. Savini reports personal fees from Alcon, Carl Zeiss Meditec AG, Johnson & Johnson Vision, Oculus, SIFI and Staar Surgical outside the submitted work.

Dr. Yeo reports personal fees from Alcon, Bausch and Lomb, Carl Zeiss Meditec, Kowa and Rayner outside of the submitted work. He is also a consultant for Bausch and Lomb and Carl Zeiss Meditec outside of the submitted work. Dr. Yeo licenses his EVO formula to Bausch and Lomb.

Dr. Taneri received speaker's honoraria from AddVision.

The remaining authors have no financial or proprietary interest in the materials presented herein.

Table of contents statement

This retrospective single-center study explores factors influencing phakic intraocular lens (pIOL) power calculations in myopic eyes. Analyzing various effective lens position algorithms, including fixed constant and linear regression models, the study incorporates posterior corneal curvature and postoperative vault. Findings reveal improved accuracy with linear regression models, especially for lower to medium power pIOLs. Clinical implications underscore enhanced refractive outcomes, recommending the LION 1_{ICL} and LION 1_{IPCL} formulas for specific pIOL platforms.